

Bethe stopping-power formula for structured projectiles

E. J. McGuire

Sandia National Laboratories, Division 9571, Albuquerque, New Mexico 87185-1187

(Received 26 February 1997)

It is known that the energy loss in ion-atom collisions is dominated by elastic scattering of one collision partner and excitation or ionization of the second. This is true for both structured and structureless projectiles. Here, I show that this fact leads to a relatively simple extension of the Bethe stopping-power formula for structureless projectiles to structured projectiles. The formula replaces the Bethe mean excitation energy with two other mean energies which reflect the elastic scattering factor of the otherwise structureless projectile. The expression is symmetrical in the center-of-mass system. The formula is in excellent agreement with numerical calculations, when the numerical calculations are asymptotic. To obtain the extended Bethe stopping formula, it is necessary to evaluate integrals over energy and momentum transfer involving generalized oscillator strengths, properly treating the energy-dependent lower limit in the momentum transfer integral. I do this by a constructive procedure using two cutoffs (instead of the traditional one) in momentum transfer. Peek had earlier developed a procedure to address the question of whether the Bethe mean excitation energy calculated with optical oscillator strengths is the same as the Bethe mean excitation energy appearing in the stopping power formula. I show that the result of the constructive procedure agrees with the result of Peek in the asymptotic limit, and I develop a criterion to determine the asymptotic limit. [S1050-2947(98)05304-9]

PACS number(s): 34.50.Bw, 34.10.+x

I. INTRODUCTION

Stopping-power (SP) measurements on thin solids with an accuracy of better than 1% have shown significant, and as yet unexplained, differences between the Bethe [1] mean excitation energy (I) calculated from atomic optical oscillator strengths [2–4] (OOS) or extracted from SP calculations using the generalized oscillator strength (GOS) formulation of the plane wave Born approximation (PWBA), and that inferred from measurements on solids [5–7]. For example, with OOS one finds $I \approx 124$ eV for Al [2–4], with the GOS one finds $I \approx 132$ eV for Al [8], while the value inferred from thin foil measurements is $I \approx 163$ – 165 eV [5–7]. A possible explanation for the discrepancy is that the I value calculated with the OOS is not the I value of a SP experiment. In the course of analyzing explicit PWBA subshell stopping-power calculations [4,8], two features stood out. First, as illustrated in Figs. (9)–(11) of Ref. [9], for $4f$ and $5d$ subshells, the OOS is often not a good approximation to the GOS for $q^2 \leq E_{nl}$, where E_{nl} is the subshell ionization energy and q is the momentum transfer, both in Rydberg units. Second, with the leading term in the subshell SP of the form $Z(nl)\ln(4m_e E_p/M_p)$, it proved impossible to fit the calculations with either the choice $Z(nl) = Z_{nl}(0)$, the subshell OOS summed over excited states (unoccupied or partially filled subshells), or with $Z(nl) = N_{nl}$, the subshell occupation number. The fitted $Z(nl)$ was generally close to $\frac{1}{2}[Z_{nl}(0) + N_{nl}]$. Just such a factor had been found earlier by Bethe *et al.* [10]. The difficulty with using $Z(nl) = \frac{1}{2}[Z_{nl}(0) + N_{nl}]$ is that $Z_{nl}(0)$ is relevant to small momentum transfer collisions and N_{nl} to large momentum transfer collisions. Then if one applies a traditional analysis, such as that of Dalgarno [11], to the subshell SP, the SP is proportional to

$$N_{nl} \ln(2km_e/Mq_{nl}) + Z_{nl}(0) \ln[(h/2\pi)^2 kq_{nl}/MI_{nl}], \quad (1a)$$

where M is the reduced mass; the Bethe mean excitation energy for the subshell is defined by

$$Z_{nl}(0) \ln(I_{nl}) = \left(\sum + \int d\varepsilon \right) \frac{d}{d\varepsilon} f(\varepsilon, 0) \ln(E_{nl} + \varepsilon). \quad (1b)$$

$(hk/2\pi)^2 = 2m_e E_p$, with E_p the projectile energy, and q_{nl} is a momentum cutoff given by

$$(hq_{nl}/2\pi)^2 = 2m_e E_{nl}. \quad (1c)$$

The definition of the cutoff used here differs from Dalgarno's [11] Eq. (13) by the use of m_e in place of the reduced mass M . At the cutoff the squared momentum transfer equals the subshell ionization energy, in Rydberg units. If q_{nl} were much larger than this, one could not approximate the GOS at small q^2 with the OOS in Eq. (1b) (which, in any case, is a dubious approximation if the OOS is a poor approximation for $q < q_{nl}$). The one-electron GOS for ionization per nl electron per $\varepsilon l'$ continuum hole is defined by

$$\frac{d}{d\varepsilon} f_{nl}(\varepsilon, q^2, l') = [(E_{nl} + \varepsilon)/q^2] | \langle nl | \exp(i\vec{q} \cdot \vec{r}) | \varepsilon l' \rangle |^2 \quad (1d)$$

with a similar definition for the excitation GOS. If one makes the further assumption that $N_{nl} = Z_{nl}(0) = Z_{nl}$, Eq. (1a) simplifies to

$$Z_{nl} \ln[2(h/2\pi)^2 k^2/M^2 I_{nl}] = Z_{nl} \ln(4E_p m_e/M_p I_{nl}), \quad (1e)$$

where the cutoffs drop out of the final result. Further, with

$$Z \ln(I) = \sum_{nl} Z_{nl}(0) \ln(I_{nl}) \quad (1f)$$

one defines the Bethe mean excitation energy based on OOS.

However, not only is the OOS not a good approximation to the GOS for $q^2 \leq E_{nl}$, but, in general, $Z_{nl}(0) \neq N_{nl}$, with the difference particularly large for d and f subshells. Then Eq. (1a) becomes

$$\begin{aligned} & \frac{1}{2}[N_{nl} + Z_{nl}(0)] \ln(4E_p m_e / M_p I_{nl}) \\ & + \frac{1}{2}[N_{nl} - Z_{nl}(0)] \ln[2m_e I_{nl} / (h q_{nl} / 2\pi)^2]. \end{aligned} \quad (2a)$$

On summing Eq. (2a) over subshells, one has in place of Eqs. (1d) and (1e)

$$\begin{aligned} & Z \ln(4E_p m_e / M_p I) + \frac{1}{2} \sum_{nl} [N_{nl} - Z_{nl}(0)] \ln(4E_p m_e / M_p I_{nl}) \\ & + \frac{1}{2} \sum_{nl} [N_{nl} - Z_{nl}(0)] \ln[2m_e I_{nl} / (h q_{nl} / 2\pi)^2] \\ & = Z \ln(4E_p m_e / M_p I) + \frac{1}{2} \sum_{nl} [N_{nl} - Z_{nl}(0)] \\ & \quad \times \ln(4E_p m_e / M_p E_{nl}). \end{aligned} \quad (2b)$$

Unless it can be shown that the second term in Eq. (2b) vanishes, it will contribute an additional term to the Bethe mean excitation energy.

Bethe *et al.* [10] did discuss but did not evaluate the additional term in Eq. (2b). Peek [12] continued the analysis of Ref. [10], and in a tour-de-force, used distribution theory to evaluate the finite part of divergent integrals, and avoiding momentum cutoffs, explicit asymptotic limits, or any discussion of the interchange of limits of energy and momentum integrals, concluded that the second term in Eq. (2b) does vanish. Peek's [12] analysis indicates that subshell I values, I_{nl} , may be changed significantly from those calculated with the OOS, but that the I value in the Bethe formula is the I value obtained by summing over subshell contributions calculated with the OOS.

Peek's [12] analysis did not examine changes in the shell corrections. In attempting to verify inner-shell corrections from explicit PWBA calculations to apply to experiment, one wants accurate subshell I values from the asymptotic theory, and some indication when asymptotia is reached. This is done here. In addition, to determine analytic approximations for the asymptotic energy loss when the projectile is structured, one begins with an extended version of the Born approximation for unstructured projectiles. It is clear that the proper approach in either case is that introduced by Bethe *et al.* [10] and continued by Peek [12]: the use of a q^2 -dependent subshell sum rule. However, one wants a constructive formalism in place of the analysis Peek [12] did using distribution theory. In Sec. II I develop an asymptotic analysis of SP using two (rather than one) momentum cutoffs to accurately represent the physics of the GOS. I confirm Peek's [12] conclusions, that even when one includes in the analysis $Z_{nl}(0) \neq N_{nl}$, and rapid changes of the GOS with squared momentum transfer, q^2 , near $q^2=0$, the atomic I value calculated with OOS is the Bethe mean excitation energy. In Sec. II assertions are made that certain parameters in the analysis are large and small enough that an asymptotic approximation applies. In Sec. III these assertions are exam-

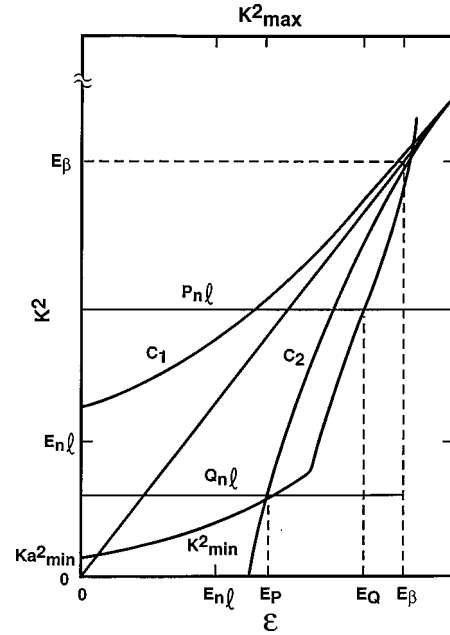


FIG. 1. Sketch of the region of the $\varepsilon - K^2$ plane between the curves C_1 and C_2 where the GOS is significant. At large ε the GOS is peaked on the Bethe ridge, where $\varepsilon = K^2$. The cutoffs discussed in Sec. II are P_{nl} and Q_{nl} . At $Q_{nl}(P_{nl}) = (K^2)_{\min}$, one has $\varepsilon_P = (4m_e E_p Q_{nl} / M_p)^{1/2}$, $[\varepsilon_P = (4m_e E_p P_{nl} / M_p)^{1/2}]$. At E_β , $(K^2)_{\min}$ intersects the Bethe ridge and $E_\beta = (4m_e E_p / M_p) - E_{nl} + 2(m_e E_p / M_p)[(1 - M_p E_{nl} / m_e E_p)^{1/2} - 1] \sim 4m_e E_p / M_p$.

ined for the case of Al. In Sec. IV the analysis of Sec. II is extended to the case of a structured projectile, leading to an extended Bethe formula. In Sec. V the extended Bethe formula is compared with PWBA calculations for Li ions incident on neutral Zn and Au. A discussion of other efforts to generalize the Bethe formulas is given in Sec. VI. The conclusions are in Sec. VII.

II. THE EFFECT OF A q^2 -DEPENDENT GOS SUM RULE

The contribution of electrons in the nl subshell to proton stopping power can be written in terms of the GOS as

$$-(1/n) \left. \frac{dE}{dx} \right|_{nl} = [4\pi(a_0)^2 (M_p / m_e) / E_p] B_{nl}, \quad (3a)$$

where

$$\begin{aligned} B_{nl} = & \sum_{n'l'} \int_{K_{\min}^2}^{K_{\max}^2} (dq^2 / q^2) f_{nl,n'l'}(q^2) \\ & + \int_0^{E_p - E_{nl}} d\varepsilon \int_{K_{\min}^2}^{K_{\max}^2} (dq^2 / q^2) \frac{d}{d\varepsilon} f_{nl}(\varepsilon, q^2), \end{aligned} \quad (3b)$$

where E_p and M_p are the proton energy and mass, E_{nl} is the subshell ionization energy, $f_{nl,n'l'}(q^2)$ is the calculated GOS from occupied or partially occupied level, nl , to partially occupied or unoccupied level, $n'l'$, and

$$K^2|_{\max, \min} = (M_p / m_e) \{ (E_p)^{1/2} \pm [E_p - \Delta E_{nl}]^{1/2} \}^2, \quad (3c)$$

with $\Delta E_{nl} = E_{n'l'} - E_{nl}$ for excitation and $\Delta E_{nl} = |E_{nl}| + \varepsilon$ for ionization. All energies and squared momentum transfers are in Rydbergs. If, for fixed q^2 , one sums the GOS over unoccupied or partially unoccupied subshells, one has the subshell GOS sum rule:

$$Z_{nl}(q^2) = \sum_{n'l'} f_{nl,n'l'}(q^2) + \int_0^\infty d\varepsilon \frac{d}{d\varepsilon} f_{nl}(\varepsilon, q^2) \quad (4a)$$

$$= N_{nl} + \sum_{n'l' < nl} |f_{nl,n'l'}^0(q^2)| - \sum_{n'l' > nl} |f_{nl,n'l'}^0(q^2)| \quad (4b)$$

$$= N_{nl} - \sum_{n'l' < nl} f_{nl,n'l'}^0(q^2) - \sum_{n'l' > nl} f_{nl,n'l'}^0(q^2) \quad (4c)$$

where $f_{nl,n'l'}^0(q^2)$ is the GOS to fully or partially occupied levels, and the sum in Eq. (4a) includes partially and fully empty subshells, only. The transitions in Eqs. (4b) and (4c) are forbidden by the Pauli principle (the FOS). Since the GOS depends on the energy difference in the transition, the

forbidden transitions either add to the right-hand side (RHS) of Eq. (4a), if $E_{n'l'} \leq E_{nl}$, or subtract if $E_{n'l'} \geq E_{nl}$.

The cutoffs $Q_{nl} = \alpha_{nl} E_{nl}$ and $P_{nl} = \beta_{nl} E_{nl}$ are introduced as illustrated in Fig. 1. The upper cutoff P_{nl} is chosen so that, for $q^2 \geq P_{nl}$, $Z_{nl}(q^2) = N_{nl}$. In Fig. 1 the curves C_1 and C_2 define the region in (ε, q^2) space where the GOS is significantly different from zero. Q_{nl} is defined as that value of q^2 at which $K_{\min}^2 = C_2$ and which simultaneously satisfies the condition

$$[f_{nl}(\varepsilon, q^2) - f_{nl}(\varepsilon, 0)] / [f_{nl}(\varepsilon, 0)] \leq \delta, \quad (5a)$$

where δ is a small parameter, such that a Taylor series expansion can be made. The value of q^2 at which $K_{\min}^2 = C_2$ is determined approximately by K_{\min}^2 evaluated at that ε value where C_2 crosses the $q^2 = 0$ axis, say $M_{nl} E_{nl}$. Then

$$Q_{nl} = (M_p / m_e) (M_{nl} + 1)^2 (E_{nl})^2 / E_p. \quad (5b)$$

For any choice of δ one can choose sufficiently large E_p such that Q_{nl} simultaneously satisfies both conditions.

Where $K_{\min}^2(\varepsilon)$ crosses the Bethe ridge (see Fig. 1), at $\varepsilon \rightarrow E_\beta = 4m_e E_p / M_p$ defines a new K_{\max}^2 , Eq. (3b) becomes

$$\begin{aligned} B_{nl} = & \int_{P_{nl}}^{E_\beta} (dq^2/q^2) \left\{ \sum_{n'l'} f_{nl,n'l'}(q^2) + \int_0^{E_p - E_{nl}} d\varepsilon \frac{d}{d\varepsilon} f_{nl}(\varepsilon, q^2) \right\} + \int_{Q_{nl}}^{P_{nl}} (dq^2/q^2) \left\{ \sum_{n'l'} f_{nl,n'l'}(q^2) \right. \\ & + \left. \int_0^{E_p - E_{nl}} d\varepsilon \frac{d}{d\varepsilon} f_{nl}(\varepsilon, q^2) \right\} + \sum_{n'l'} \int_{K_{\min}^2}^{Q_{nl}} (dq^2/q^2) \left[f_{nl,n'l'}(0) + q^2 \frac{d}{dq^2} f_{nl,n'l'}(q^2) \right] \Big|_{q^2=0} \\ & + \left. \int_0^{E_p - E_{nl}} d\varepsilon \int_{K_{\min}^2}^{Q_{nl}} (dq^2/q^2) \left\{ \frac{d}{d\varepsilon} f_{nl}(\varepsilon, 0) + q^2 \frac{d}{dq^2} \left[\frac{d}{d\varepsilon} f_{nl}(\varepsilon, q^2) \right] \right\} \right] \Big|_{q^2=0}. \end{aligned} \quad (6a)$$

For the first term in Eq. (6a) the sum and integral in curly brackets is N_{nl} by the definition of P_{nl} , while the second term in curly brackets in Eq. (6a) is $Z_{nl}(q^2)$. The third term is

$$\sum_{n'l'} \left[f_{nl,n'l'}(0) \ln(Q_{nl}/K_{\min}^2) + (Q_{nl} - K_{\min}^2) \frac{d}{dq^2} f_{nl,n'l'}(q^2) \right] \Big|_{q^2=0}. \quad (6b)$$

Since both Q_{nl} and K_{\min}^2 are proportional to $1/E_p$, the integral over ε of terms proportional to $(Q_{nl} - K_{\min}^2) df/dq^2$ can be neglected to order $(1/E_p)$. Thus we drop the second term in Eq. (6b). A similar argument applies to the fourth term in Eq. (6a), and with the limit $E_p - E_{nl}$ in the fourth term replaced by $\varepsilon_p = (4m_e E_p Q_{nl} / M_p)^{1/2}$ (where $K_{\min}^2 = Q_{nl}$), Eq. (6a) becomes

$$B_{nl} = N_{nl} \int_{P_{nl}}^{E_\beta} dq^2/q^2 + \int_{Q_{nl}}^{P_{nl}} (dq^2/q^2) Z_{nl}(q^2) + \sum_{n'l'} f_{nl,n'l'}(0) \ln(Q_{nl}/K_{\min}^2) + \int_0^{\varepsilon_p} d\varepsilon \frac{d}{d\varepsilon} f_{nl}(\varepsilon, 0) \ln(Q_{nl}/K_{\min}^2) \quad (6c)$$

or

$$B_{nl} = N_{nl} \ln[4m_e E_p / M_p P_{nl}] + \int_{Q_{nl}}^{P_{nl}} (dq^2/q^2) Z_{nl}(q^2) + Z_{nl}(0) \ln\{4m_e E_p Q_{nl} / [M_p (I_{nl}^{\text{op}})^2]\}, \quad (6d)$$

where the I value based on optical oscillator strength is defined by

$$Z_{nl}(0) \ln(I_{nl}^{\text{op}}) = \sum_{n'l'} f_{nl,n'l'}(0) \ln(E_{n'l'} - E_{nl}) + \int_0^{\varepsilon_p} d\varepsilon \frac{d}{d\varepsilon} f_{nl}(\varepsilon, 0) (E_{nl} + \varepsilon). \quad (6e)$$

Using Eq. (4b) one has for Eq. (6d) [replacing $Z_{nl}(q^2)$ with N_{nl} plus a correction]

$$\begin{aligned}
B_{nl} &= N_{nl} [\ln(4m_e E_p / M_p P_{nl}) + \ln(P_{nl} / Q_{nl})] + Z_{nl}(0) \ln\{4m_e E_p Q_{nl} / [M_p (I_{nl}^{\text{op}})^2]\} \\
&+ \int_{Q_{nl}}^{P_{nl}} dq^2 / q^2 \left\{ \sum_{n'l' < nl} \left| f_{nl, n'l'}^0(q^2) \right| - \sum_{n'l' > nl} \left| f_{nl, n'l'}^0(q^2) \right| \right\} \\
&= [Z_{nl}(0) + N_{nl}] \ln(4m_e E_p / M_p I_{nl}^{\text{op}}) + [N_{nl} - Z_{nl}(0)] \ln(I_{nl}^{\text{op}} / Q_{nl}) \\
&+ \int_{Q_{nl}}^{P_{nl}} (dq^2 / q^2) \left\{ \sum_{n'l' < nl} \left| f_{nl, n'l'}^0(q^2) \right| - \sum_{n'l' > nl} \left| f_{nl, n'l'}^0(q^2) \right| \right\}. \tag{6f}
\end{aligned}$$

The first term in Eq. (6f) is that which was obtained by Bethe *et al.* [10], the second term is the effect of the difference between the summed OOS and the occupation number; it also depends on the choice of low momentum transfer cutoff. The third term is a consequence of the forbidden GOS created by the Pauli exclusion principle; its contribution would be zero if $P_{nl} = Q_{nl}$. These additional terms contribute to an effective subshell Bethe mean excitation energy, I_{nl} :

$$\begin{aligned}
-[Z_{nl}(0) + N_{nl}] \ln(I_{nl}) &= -[Z_{nl}(0) + N_{nl}] \ln(I_{nl}^{\text{op}}) + [N_{nl} - Z_{nl}(0)] \ln(I_{nl}^{\text{op}} / Q_{nl}) \\
&+ \int_{Q_{nl}}^{P_{nl}} (dq^2 / q^2) \left\{ \sum_{n'l' < nl} \left| f_{nl, n'l'}^0(q^2) \right| - \sum_{n'l' > nl} \left| f_{nl, n'l'}^0(q^2) \right| \right\}, \tag{6g}
\end{aligned}$$

where I_{nl}^{op} is determined by the OOS in Eq. (6d).

If one averages over initial states and sums over final states then

$$f_{nl, n'l'}^0(q^2) = -f_{n'l', nl}^0(q^2), \tag{7a}$$

which is not immediately obvious, since there is no involvement of statistical weights in Eq. (7a). To demonstrate its validity, consider that R is the GOS from a filled subshell (1), with n_{10} electrons to an empty subshell (2), with n_{20} holes. For the transition from a filled (2) subshell to an empty (1) subshell the GOS is $-R$, since in both cases the initial term is a 1S . For a transition from a partially filled (1)

subshell with n_1 of n_{10} electrons to a partially filled (2) subshell with n_2 of n_{20} electrons, the GOS is $R(n_1/n_{10})(n_{20} - n_2)/n_{20}$. But the part of the GOS lost due to the Pauli principle is that due to the partial occupancy of the final level. If (2) were unoccupied the GOS would be $R(n_1/n_{10})$, so the forbidden GOS is $R(n_1/n_{10})(n_2/n_{20})$. The result is symmetrical in (1) and (2); for the reverse transition one finds the same result with a minus sign. This justifies Eq. (7a), and Eq. (7a) ensures that the GOS sum rule is preserved in Eq. (4b) since if n_0 is the outermost partially occupied level, and we sum over nl for occupied and partially occupied shells,

$$\begin{aligned}
\sum_{n=1, l=0}^{n_0} \left[\sum_{n'l' < nl} \left| f_{nl, n'l'}^0(q^2) \right| - \sum_{n'l' > nl} \left| f_{nl, n'l'}^0(q^2) \right| \right] &= \sum_{n=1, l=0}^{n_0} \sum_{n'l' < nl} |f_{nl, n'l'}^0(q^2)| - \sum_{n=1, l=0}^{n_0} \sum_{n'l' > nl} |f_{nl, n'l'}^0(q^2)| \\
&= \sum_{n=2, l=0}^{n_0} \sum_{n'l' < nl} |f_{nl, n'l'}^0(q^2)| - \sum_{n=1, l=0}^{n_0-1} \sum_{n'l' > nl} |f_{nl, n'l'}^0(q^2)|. \tag{7b}
\end{aligned}$$

But by Eq. (7a)

$$\sum_{n=2, l=0}^{n_0} \sum_{n'l' < nl} |f_{nl, n'l'}^0(q^2)| = \sum_{n=2, l=0}^{n_0} \sum_{n'l' < nl} |f_{n'l', nl}^0(q^2)| = \sum_{n'=1, l'=0}^{n_0-1} \sum_{nl > n'l'} |f_{n'l', nl}^0(q^2)|, \tag{7c}$$

which by an interchange of summation variables is

$$\sum_{n=2, l=0}^{n_0} \sum_{n'l' < nl} |f_{nl, n'l'}^0(q^2)| = \sum_{n=1, l=0}^{n_0-1} \sum_{n'l' > nl} |f_{nl, n'l'}^0(q^2)| \tag{7d}$$

so that Eq. (7b) reduces to zero.

We can rewrite Eq. (6g) as

$$\begin{aligned}
 -[Z_{nl}(0) + N_{nl}]\ln(I_{nl}) &= -[Z_{nl}(0) + N_{nl}]\ln(I_{nl}^{op}) + [N_{nl} - Z_{nl}(0)]\ln(I_{nl}^{op}/Q_{nl}) \\
 &+ \left[- \sum_{n'l' < nl} f_{n'l',nl}^0(0) + \sum_{n'l' > nl} f_{nl,n'l'}^0(0) \right] \ln(I_{nl}^{op}/Q_{nl}) \\
 &+ \int_{Q_{nl}}^{P_{nl}} (dq^2/q^2) \left\{ \sum_{n'l' < nl} f_{n'l',nl}^0(q^2) - \sum_{n'l' > nl} f_{nl,n'l'}^0(q^2) \right\}, \tag{8a}
 \end{aligned}$$

where all the FOS are now positive. First, I examine dipole allowed FOS, where $f_{nl,n'l'}^0(0) \neq 0$, where there is a scale parameter determined by the more negative energy in the transition, i.e.,

$$f_{n'l',nl}^0(q^2) = f_{n'l',nl}^0(q^2/E_{n'l'}) \tag{8b}$$

so that for dipole allowed transitions

$$f_{n'l',nl}^0(q^2) = f_{n'l',nl}^0(0) [f_{n'l',nl}^0(q^2/E_{n'l'}) / (f_{n'l',nl}^0(0))]. \tag{8c}$$

Then

$$-[Z_{nl}(0) + N_{nl}]\ln(I_{nl}) = -[Z_{nl}(0) + N_{nl}]\ln(I_{nl}^{op}) + B_{nl}^D, \tag{9a}$$

where

$$\begin{aligned}
 B_{nl}^D &= - \sum_{n'l' < nl} f_{n'l',nl}^0(0) \ln\{I_{nl}^{op} / [E_{n'l'} T(n'l', nl, P_{nl}/E_{n'l'}, Q_{nl}/E_{n'l'})]\} \\
 &+ \sum_{n'l' > nl} f_{nl,n'l'}^0(0) \ln\{I_{nl}^{op} / [E_{nl} T(nl, n'l', P_{nl}/E_{nl}, Q_{nl}/E_{nl})]\} \tag{9b}
 \end{aligned}$$

with

$$T_2(y) = \int_1^y (dz/z) \{ f_{n'l',nl}^0(z) / [f_{n'l',nl}^0(0)] - 1 \} + \ln(y). \tag{9e}$$

$$\begin{aligned}
 T(n'l', nl, y, x) &= \ln(x) + \int_x^y (dz/z) \{ f_{n'l',nl}^0(z) / [f_{n'l',nl}^0(0)] \} \\
 &= T_1(x) + T_2(y), \tag{9c}
 \end{aligned}$$

where

$$T_1(x) = \int_x^1 (dz/z) [f_{n'l',nl}^0(z) / (f_{n'l',nl}^0(0)) - 1] \tag{9d}$$

and

Because $f_{n'l',nl}^0(z)$ decreases rapidly as $z \rightarrow \infty$, $\ln[T(n'l', nl, y, x)]$ will be independent of y , if $y = P_{nl}/E_{n'l'}$ is sufficiently large, i.e., $T_2(y)$ approaches a constant as y increases. Similarly, one expects $\ln[T(n'l', nl, y, x)]$ to be independent of x , if $x = Q_{nl}/E_{nl} = (M_P/4m_e)(M_{nl} + 1)^2 E_{nl}/E_P$ is sufficiently small, i.e., $T_1(x)$ approaches a constant as x goes to zero. Clearly such choices (sufficiently small, sufficiently large) can be asserted in an analytic theory; in numerical calculations and experiment one needs to know when these asymptotic limits are reached. I return to this point in the next section.

Assuming the asymptotic criteria have been satisfied one can write Eq. (9b) as

$$\begin{aligned}
 B_{nl}^D &= - \sum_{n'l' < nl} f_{n'l',nl}^0(0) \ln\{I_{nl}^{op} / [E_{n'l'} T(n'l', nl)]\} + \sum_{n'l' > nl} f_{nl,n'l'}^0(0) \ln\{I_{nl}^{op} / [E_{nl} T(nl, n'l')]\} \\
 &- \sum_{n'l' > nl} f_{nl,n'l'}^0(0) \ln\{I_{n'l'}^{op} / [E_{nl} T(nl, n'l')]\} + \sum_{n'l' > nl} f_{nl,n'l'}^0(0) \ln\{I_{nl}^{op} / [E_{nl} T(nl, n'l')]\} \\
 &= \sum_{n'l' > nl} f_{nl,n'l'}^0(0) \ln(I_{nl}^{op} / I_{n'l'}^{op}). \tag{10}
 \end{aligned}$$

Then in the asymptotic limit

$$-[Z_{nl}(0) + N_{nl}]\ln(I_{nl}) = -[Z_{nl}(0) + N_{nl}]\ln(I_{nl}^{\text{op}}) + \sum_{n'l' > nl} f_{nl,n'l'}^0(0)\ln(I_{nl}^{\text{op}}/I_{n'l'}^{\text{op}}) \quad (11a)$$

and if we sum over nl , we have

$$2Z \ln(I) = \sum_{nl} [Z_{nl}(0) + N_{nl}]\ln(I_{nl}) = \sum_{nl} [Z_{nl}(0) + N_{nl}]\ln(I_{nl}^{\text{op}}) - \sum_{nl} \sum_{n'l' > nl} f_{nl,n'l'}^0(0)\ln(I_{nl}^{\text{op}}/I_{n'l'}^{\text{op}}). \quad (11b)$$

Expressing $Z_{nl}(0)$ in terms of the FOS one finds

$$2Z \ln(I) = 2 \sum_{nl} N_{nl} \ln(I_{nl}^{\text{op}}) + \sum_{nl} \left[\sum_{n'l' < nl} f_{n'l',nl}^0(0) - \sum_{n'l' > nl} f_{nl,n'l'}^0(0) \right] \ln(I_{nl}^{\text{op}}) - \sum_{nl} \sum_{n'l' > nl} f_{nl,n'l'}^0(0)\ln(I_{nl}^{\text{op}}/I_{n'l'}^{\text{op}}), \quad (11c)$$

which with an obvious interchange of variables becomes

$$2Z \ln(I) = 2 \sum_{nl} \ln(I_{nl}^{\text{op}}) \left[N_{nl} + \sum_{n'l' < nl} f_{n'l',nl}^0(0) - \sum_{n'l' > nl} f_{nl,n'l'}^0(0) \right] = 2 \sum_{nl} Z_{nl}(0) \ln(I_{nl}^{\text{op}}). \quad (11d)$$

Thus the Bethe mean excitation energy is identical to the Bethe mean excitation energy calculated with optical oscillator strengths as first demonstrated by Peek [12].

The nondipole terms in the FOS contribute a correction, B_{nl}^Q , to the RHS of Eq. (8a), given by

$$B_{nl}^Q = \int_{K_{\min}^2}^{P_{nl}} (dq^2/q^2) \left\{ \sum_{n'l' < nl} f_{n'l',nl}^{\text{ond}}(q^2) - \sum_{n'l' > nl} f_{nl,n'l'}^{\text{ond}}(q^2) \right\}, \quad (12a)$$

where scaling is assumed

$$f_{n'l',nl}^{\text{ond}}(q^2) = f_{n'l',nl}^{\text{ond}}(q^2/E_{n'l'}). \quad (12b)$$

Since

$$f_{n'l',nl}^{\text{ond}}(0) = 0, \quad (12c)$$

I continue the analysis with $f_{nl,n'l'}^{\text{ond}}(q^2)|_{\max} = f_{nl,n'l'}^{\text{ond}}|_{\max}$, rather than with $f_{n'l',nl}^{\text{ond}}(0)$. Then

$$B_{nl}^Q = \sum_{n'l' < nl} f_{n'l',nl}^{\text{ond}}(q^2)|_{\max} Q(n'l', nl, P_{nl}/E_{n'l'}) - \sum_{n'l' > nl} f_{nl,n'l'}^{\text{ond}}|_{\max} Q(nl, n'l', P_{nl}/E_{nl}), \quad (13a)$$

where

$$Q(n'l', nl, x) = \int_0^x (dy/y) [f_{n'l',nl}^{\text{ond}}(y)/f_{n'l',nl}^{\text{ond}}(y)|_{\max}]. \quad (13b)$$

In Eq. (13b) I have set the lower limit to zero since the nondipole FOS is zero in this limit. Since the nondipole FOS drops off rapidly with large y , there is some $x(P_{nl})$ above

which $Q(n'l', nl, x)$ is unchanging. In this asymptotic limit where $Q(n'l', nl, x) = Q(n'l', nl, \infty)$,

$$B_{nl}^Q = \sum_{n'l' < nl} f_{n'l',nl}^{\text{ond}}|_{\max} Q(n'l', nl, \infty) - \sum_{n'l' > nl} f_{nl,n'l'}^{\text{ond}}|_{\max} Q(nl, n'l', \infty), \quad (14)$$

which vanishes when one interchanges primed and unprimed indices in one of the above sums, completing the proof of Eq. (11d).

III. THE ASYMPTOTIC LIMITS IN Al

To illustrate the asymptotic limits assumed in Sec. II, in Fig. 2(a) I show the calculated dipole FOS ratio, $f_{n'l',nl}^0(x)/[f_{n'l',nl}^0(0)]$ for transitions in neutral Al, where $x = q^2/E_{nl}$. The shapes vary from transition to transition, with zeros occurring as a function of $x = q^2/E_{nl}$ for the $2s-3p$ and $2p-3s$ transitions. In Fig. 2(b) I show $T_1(x)$ versus x for the six Al dipole transitions; it is clear that $T_1(x)$ saturates for $x \leq 0.01$. In Fig. 2(c) I show $T_2(x)$ versus x , which saturates for $x \geq 10$. These are sufficient conditions for the validity of the asymptotic approximation. From Eq. (5b) the condition $Q_{nl}/E_{nl} \leq 0.01$ requires

$$Q_{nl}/E_{nl} = (M_p/m_e)(M_{nl} + 1)^2 E_{nl}/E_p \leq 0.01 \quad (15a)$$

or

$$E_p \geq 100(M_p/m_e)(M_{nl} + 1)^2 E_{nl}. \quad (15b)$$

For Al with $M_{1s} = 3$ and $E_{1s} = 112$ Ry, the sufficiency condition in Eq. (15b) is $E_p > 10^9$ eV.

In Fig. 3 I show $f_{n'l',nl}^{\text{ond}}(y)/f_{n'l',nl}^{\text{ond}}(y)|_{\max}$ for the monopole FOS in Al, where $x = q^2/E_{nl}$. The points are explicit calculations while the solid curve is a rough universal fit. The integral is discussed in the Appendix. For $P_{nl} > 4E_{n'l'}$, $W(n'l', nl, x) = 3.15$ (but not π).

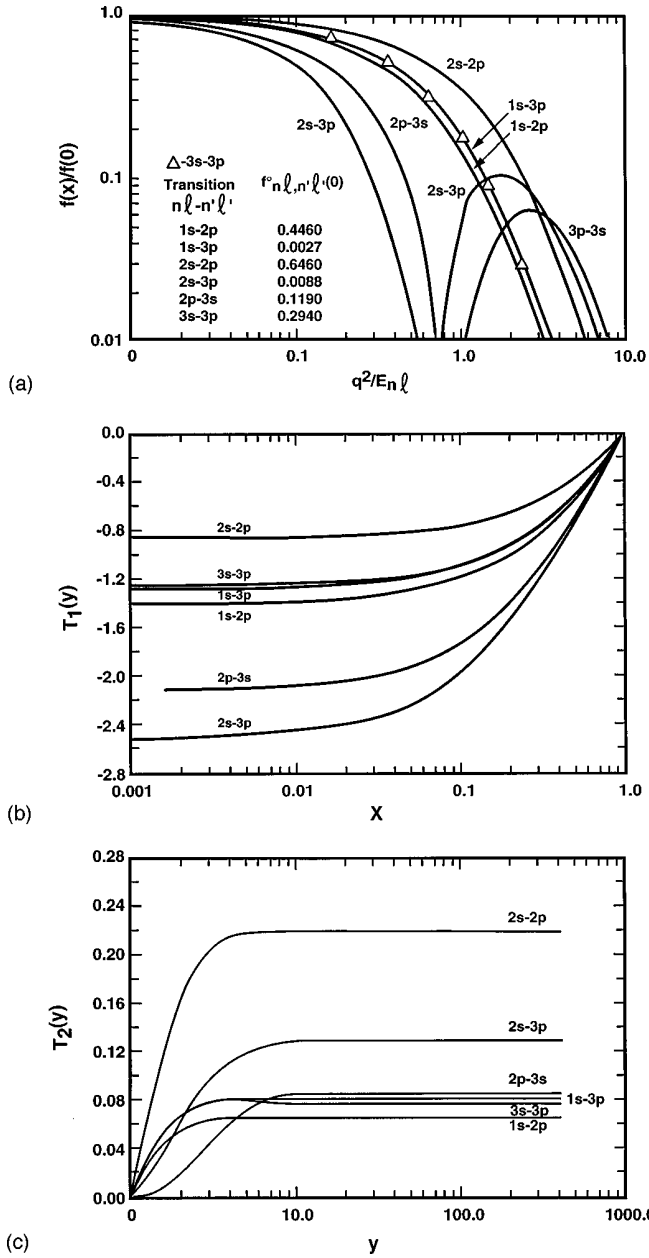


FIG. 2. (a) Calculated Al dipole GOS shapes for transitions forbidden by the Pauli exclusion principle (FOS). The normalizing values (at $q^2=0$) are tabulated. The 1s-3p and 3s-3p shapes are almost identical. (b) The integral $T_1(x)$ of Eq. (9d) for the dipole FOS of Fig. (2a) showing the saturation as $x \rightarrow 0$. (c) The integral $T_2(x)$ of Eq. (9e) for the dipole FOS of Fig. (2a) showing the saturation as $y \rightarrow \infty$.

IV. THE ASYMPTOTIC ENERGY LOSS IN STRUCTURED ION COLLISIONS

When the projectile in a collision carries electrons an additional energy loss can occur due to excitation and ionization of the projectile. In the center-of-mass system (CM) the energy loss expression is symmetrical in the two collision partners. At high energy the dominant contributions to energy loss arise from elastic scattering of one partner and ionization (and, to a lesser extent, excitation) of the other projectile [13]. In the CM system the contribution to energy

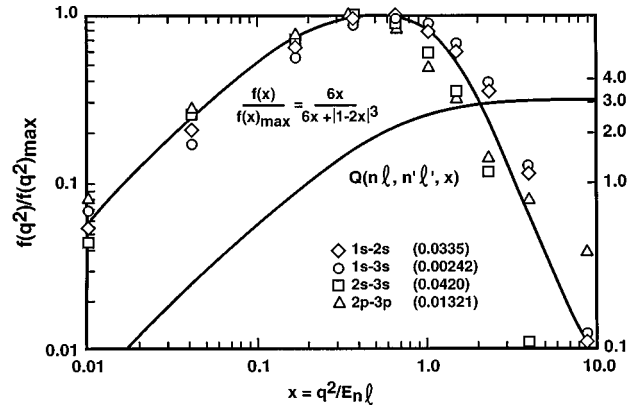


FIG. 3. Calculated Al monopole GOS forbidden by the Pauli exclusion principle. The points are the calculations; the unlabeled figure is the fitting function $f(x)/f(x)_{\max}$, while Q is the integral of Eq. (13b).

loss from elastic scattering of particle (a) and excitation and ionization of the nl subshell of ion (b) is

$$-(1/n) \left. \frac{dE}{dx} \right|_{es, nl} = [4\pi(a_0)^2 (M_r/m_e)/E_r] B_{es, nl}, \quad (16a)$$

where

$$B_{es, nl} = \sum_{n'l'} \int_{K_{\min}^2}^{K_{\max}^2} (dq^2/q^2) f_{nl, n'l'}(q^2) |\mathcal{F}_{ES}(q^2)|^2 + \int_0^{E_r - E_{nl}} \times d\varepsilon \int_{K_{\min}^2}^{K_{\max}^2} (dq^2/q^2) \frac{d}{d\varepsilon} f_{nl}(\varepsilon, q^2) |\mathcal{F}_{ES}(q^2)|^2, \quad (16b)$$

where M_r and E_r are the reduced mass and energy, and the elastic scattering factor \mathcal{F}_{ES} for particle (a) is

$$\mathcal{F}_{ES}(q^2) = Z_a - F_a(q^2), \quad (17a)$$

where

$$F_a(q^2) = \sum_i n_{ai} \langle ia | \exp[i\vec{q} \cdot \vec{r}] | ia \rangle \quad (17b)$$

and n_{ai} is the occupation number of the i th subshell of ion (a). For $|q| \rightarrow 0$, $F_a(q^2) \rightarrow Z_a - z_a$, and $\mathcal{F}_{ES} \rightarrow z_a$ the number of electrons on the ion, while for $|q| \rightarrow \infty$, $F_a(k^2) \rightarrow 0$, and $\mathcal{F}_{ES} \rightarrow Z_a$, the nuclear charge. Proceeding as with Eq. (6) one finds

$$B_{es,nl} = N_{nl} \int_{P_{nl}}^{E_B} (dq^2/q^2) |\mathcal{F}_{ES}(q^2)|^2 + \int_{Q_{nl}}^{P_{nl}} (dq^2/q^2) Z_{nl}(q^2) |\mathcal{F}_{ES}(q^2)|^2 + (z_a)^2 \times \left[\sum_{n'l'} f_{nl,n'l'}(0) \ln(Q_{nl}/K_{\min}^2) + \int_0^{\varepsilon_P} d\varepsilon \frac{d}{d\varepsilon} f_{nl}(\varepsilon, 0) \ln(Q_{nl}/K_{\min}^2) \right] \quad (18a)$$

or

$$B_{es,nl} = N_{nl} \int_{P_{nl}}^{E_B} (dq^2/q^2) |\mathcal{F}_{ES}(q^2)|^2 + \int_{Q_{nl}}^{P_{nl}} (dq^2/q^2) Z_{nl}(q^2) |\mathcal{F}_{ES}(q^2)|^2 + (z_a)^2 Z_{nl}(0) \ln\{4m_e E_r Q_{nl} / [M_r (I_{nl}^{\text{op}})^2]\}, \quad (18b)$$

where I_{nl}^{op} is Bethe mean excitation energy calculated with optical oscillator strengths in Eq. (6e), and $E_B = 4m_e E_r / M_r$. Using Eq. (4b) one has for Eq. (18b) [replacing $Z_{nl}(q^2)$ with N_{nl} plus a correction]

$$B_{es,nl} = N_{nl} \int_{Q_{nl}}^{E_B} (dq^2/q^2) |\mathcal{F}_{ES}(q^2)|^2 + (z_a)^2 Z_{nl}(0) \ln\{4m_e E_r Q_{nl} / [M_r (I_{nl}^{\text{op}})^2]\} + \int_{Q_{nl}}^{P_{nl}} (dq^2/q^2) |\mathcal{F}_{ES}(q^2)|^2 \left\{ \sum_{n'l' < nl} \left| f_{nl,n'l'}^0(q^2) \right| - \sum_{n'l' > nl} \left| f_{nl,n'l'}^0(q^2) \right| \right\}. \quad (18c)$$

The last term in Eq. (18c) will vanish in the asymptotic limit by the arguments given in Sec. II. Then we have

$$\begin{aligned} B_{es,nl} &= N_{nl} \int_{Q_{nl}}^{E_B} (dq^2/q^2) |\mathcal{F}_{ES}(q^2)|^2 + (z_a)^2 Z_{nl}(0) \ln[E_B Q_{nl} / (I_{nl}^{\text{op}})^2] \\ &= N_{nl} (Z_a)^2 \ln(E_B / Q_{nl}) - N_{nl} \int_{Q_{nl}}^{E_B} (dq^2/q^2) [(Z_a)^2 - |\mathcal{F}_{ES}(q^2)|^2] \\ &\quad + (z_a)^2 Z_{nl}(0) \ln[(E_B)^2 / (I_{nl}^{\text{op}})^2] - (z_a)^2 Z_{nl}(0) \ln[E_B / Q_{nl}] \\ &= [N_{nl} (Z_a)^2 - (z_a)^2 Z_{nl}(0)] \ln(E_B / Q_{nl}) + 2(z_a)^2 Z_{nl}(0) \ln[E_B / I_{nl}^{\text{op}}] - N_{nl} \int_{Q_{nl}}^{E_B} (dq^2/q^2) [(Z_a)^2 - |\mathcal{F}_{ES}(q^2)|^2]. \end{aligned} \quad (19)$$

The last term in Eq. (19) is of the form dq^2/q^2 at large q and therefore the integral will go to a constant as $E_B \rightarrow \infty$. Then

$$B_{es,nl} = [N_{nl} (Z_a)^2 - (z_a)^2 Z_{nl}(0)] \ln(E_B / I_{nl}^{es}) + 2(z_a)^2 Z_{nl}(0) \ln[E_B / I_{nl}^{\text{op}}] + [N_{nl} (Z_a)^2 - (z_a)^2 Z_{nl}(0)] \ln(I_{nl}^{es} / Q_{nl}) - N_{nl} \int_{Q_{nl}}^{E_B} (dq^2/q^2) [(Z_a)^2 - |\mathcal{F}_{ES}(q^2)|^2] \quad (20a)$$

and if we define I_{nl}^{es} by

$$[N_{nl} (Z_a)^2 - (z_a)^2 Z_{nl}(0)] \ln(I_{nl}^{es}) = [N_{nl} (Z_a)^2 - (z_a)^2 Z_{nl}(0)] \ln(Q_{nl}) + N_{nl} \int_{Q_{nl}}^{E_B} (dq^2/q^2) [(Z_a)^2 - |\mathcal{F}_{ES}(q^2)|^2] \quad (20b)$$

the second line in Eq. (20a) will vanish. Then

$$(Z_b - z_b) \ln[I(a, b, 1)] = \sum_{nl} N_{nl} \ln(I_{nl}^{es}) \quad (21a)$$

$$B_{es,nl} = [N_{nl} (Z_a)^2 - (z_a)^2 Z_{nl}(0)] \ln(E_B / I_{nl}^{es}) + 2(z_a)^2 Z_{nl}(0) \ln[E_B / I_{nl}^{\text{op}}]. \quad (20c) \quad \text{and}$$

$$(Z_b - z_b) \ln[I(a, b, 2)] = \sum_{nl} Z_{nl}(0) \ln(I_{nl}^{es}) \quad (21b)$$

If we define

TABLE I. Values of the subshell parameters $Z_{nl}(0)$ and $I_{nl}(0)$ (in eV) for Li ions, and neutral Zn and Au, calculated with optical oscillator strengths.

Level \ Ion or Atom	Li ⁺²	Li ⁺¹	Li ⁺⁰	Zn	Au
1s	1.000/135.	2.003/100.9	2.004/107.9	1.373/15950.0	1.173/103 000.0
2s			1.000/3.287	1.321/2702.0	1.119/24800.0
2p				5.411/1402.0	3.018/17890.0
3s				0.879/552.9	1.137/7196.0
3p				3.780/361.9	4.273/5362.0
3d				15.08/112.9	9.586/3583.0
4s				2.173/5.695	1.055/1918.0
4p					3.947/1630.0
4d					8.290/1220.0
4f					24.84/535.2
5s					0.643/434.7
5p					2.274/282.5
5d					16.63/45.93
6s					1.124/3.774
Total	1.000/135.0	2.003/100.9	3.004/33.74	30.03/250.5	79.11/660.6

then summing over nl leads to

$$I_b^{es} = (I_b)^2 / I(a, b, 2). \quad (23b)$$

$$B_{a,b}^{es} = \sum_{nl} B_{es,nl} = (Z_b - z_b) \{ 2(z_a)^2 \ln(4m_e E_r / M_r I_b) + (Z_a)^2 \ln[4m_e E_r / M_r I(a, b, 1)] - (z)^2 \ln[4m_e E_r / M_r I(a, b, 2)] \}, \quad (22)$$

where I_b is the Bethe mean excitation energy for ion/atom (b) given by Eq. (1e). Combining terms leads to

$$B_{a,b}^{es} = (Z_b - z_b) \{ (z_a)^2 \ln(4m_e E_r / M_r I_b^{es}) + (Z_a)^2 \ln[4m_e E_r / M_r I(a, b, 1)] \}, \quad (23a)$$

where

$$-(1/n) \left. \frac{dE}{dx} \right|_{es} = [4\pi(a_0)^2 (M_r / m_e) / E_r] (B_{a,b}^{es} + B_{b,a}^{es}) = [4\pi(a_0)^2 (M_r / m_e) / E_r] \{ (Z_b - z_b) \{ (z_a)^2 \ln(4m_e E_r / M_r I_b^{es}) + (Z_a)^2 \ln[4m_e E_r / M_r I(a, b, 1)] \} + (Z_a - z_a) \{ (z_b)^2 \ln(4m_e E_r / M_r I_a^{es}) + (Z_b)^2 \ln[4m_e E_r / M_r I(b, a, 1)] \} \}. \quad (24)$$

This formula is similar to a simpler one given in Eq. (23b) of Ref. [13]. They differ in the choice of I values in the denominators.

V. COMPARISON OF EXPLICIT CALCULATIONS AND THE EXTENDED BETHE FORMULA

For the cases of Li ions on Zn and Au treated in Ref. [13], the Bethe mean excitation energies, extracted from the explicit SP calculations for protons on Li ions, Zn, and Au,

Thus, the simple Bethe logarithm for the SP of incident structureless projectiles has been generalized to an expression involving two logarithms. Both logarithm terms are proportional to $Z_b - z_b$, the number of electrons on ion (b), while one logarithm is proportional to $(z_a)^2$ while the other term is proportional to $(Z_a)^2$, the limits of the elastic scattering factor for ion (a). The single Bethe mean excitation energy for ion (b) is replaced by a different mean excitation energy in each logarithm, both new mean excitation energies reflecting properties of both ions (a) and (b).

Of course the generalized Bethe logarithm in the energy loss expression is symmetrical in the two collision partners in the CM system and is

were 33.66, 103.6, and 141.2 eV, for Li⁺⁰, Li⁺¹, and Li⁺², respectively, and 271.2 eV for Zn and 860 eV for Au. In Table I are listed $Z_{nl}(0)$ and $I_{nl}^{op}(0)$ values for the ions and atoms calculated with optical oscillator strengths (OOS). For all the atoms or ions the summed $Z_{nl}(0)$ from the raw OOS is close to the number of electrons. For Li⁺⁰ and Li⁺¹, the total I value, extracted from the proton calculations, is in excellent agreement with the I value calculated with the OOS. For Li⁺² I use nine times the hydrogenic value of 15 eV, quoted by Dalgarno [11], for the OOS value. This is

TABLE II. Values of the subshell parameters I_{nl}^{es} calculated with the ionization energy of one ion and the modified elastic scattering factor of the other for Li ions on Zn. The generalized mean excitation energies, $I(a,b,j)$ and $I(b,a,j)$, are also listed.

Level \ Ion or atom	Li ⁺²	Zn	Li ⁺¹	Zn	Li ⁺⁰	Zn
1s	511.96	221.68	511.91	260.89	511.91	253.77
2s		115.33		191.31	511.87	164.37
2p		169.95		206.20		159.78
3s		43.43		150.27		148.73
3p		58.81		163.87		148.20
3d		27308.0		338.62		147.96
4s		372.75		227.50		147.95
$I(\dots 1)/I(\dots 2)$	511.96/ 511.96	713.13/ 1936.2	511.90/ 514.71	231.45/ 258.81	511.90/ 514.38	156.96/ 154.75

slightly smaller than the value 141.2 extracted from the explicit calculations. For Zn and Au the I values calculated with the OOS are significantly lower than the I values extracted from the explicit calculations. In Sec. III we obtained the criterion $Q_{nl}/E_{nl} \leq 0.01$ to assure that we are in the asymptotic region; I use that condition, and the E_{nl} values used in the explicit calculations [13], along with the $Z_{nl}(0)$ values in Table I, to determine I_{nl}^{es} in Eq. (20b). The calculations require elastic scattering factors and those of the explicit calculations were used [13]. The Zn elastic scattering factor is shown in Ref. [14]. In Table II I list the values of I_{nl}^{es} for each pair in the Li ion-neutral Zn collisions. Consider first the case of neutral Zn, which is elastically scattered from neutral Li, which is excited or ionized. For the eigenvalues of the 1s and 2s subshells of Li the binding energies are much less than 10 Ry, so $Q_{nl} = 0.01 E_{nl} \leq 1.0$; since the argument of the integral in Eq. (20b) is $\approx (Z_a)^2/q^2$ for small q^2 we have

$$\begin{aligned}
 & [N_{nl}(Z_a)^2 - (z_a)^2 Z_{nl}(0)] \ln(I_{nl}^{es}) \\
 &= [N_{nl}(Z_a)^2 - (z_a)^2 Z_{nl}(0)] \ln(Q_{nl}) \\
 &+ N_{nl}(Z_a)^2 \int_{Q_{nl}}^1 (dq^2/q^2) \\
 &+ N_{nl} \int_1^{E_B} (dq^2/q^2) [(Z_a)^2 - |\mathcal{F}_{ES}(q^2)|^2]. \quad (25)
 \end{aligned}$$

For $z_a = 0$, the first integral in Eq. (25) will cancel the $\ln(Q_{nl})$ term leaving only the second integral, which is independent of E_{nl} , and independent of E_B for E_B large. The I_{nl}^{es} value does depend on the elastic scattering factor. Thus for all the Li ions the I_{nl}^{es} value is 512 eV because the neutral Zn elastic scattering factor is used throughout. The same argument applies to the 3s-4s levels of Zn. For the 2s and 2p levels of Zn $Q_{nl} \approx O(1)$, and the above argument begins to break down. The same arguments apply to ions except that $z_a \neq 0$. But for $Q_{nl} \leq 1$, the $(z_a)^2 Z_{nl}(0) \ln(Q_{nl})$ term is negative, and extremely large when $Z_{nl}(0) > N_{nl}$. This is the origin of the large I_{nl}^{es} value for the 3d subshell in Table II, and accounts for the large increase in $I(b,a,1)$ and $I(b,a,2)$ for Zn as the degree of ionization of Li is increased. Explicit calculations

of the contribution of elastic scattering of one ion and ionization and excitation of the other ion to the total energy loss [13] are shown as solid lines in Fig. 4 for Li ions on Zn. The open and solid circles, triangles, and squares are obtained with Eqs. (23). For the 3 upper curves, for elastic scattering of Zn, the results with the approximate energy loss expression of Eq. (23a) (solid circles, triangles, and squares) are in excellent agreement with the numerical results above the peak in the approximate expression at 4 MeV. This should be compared with differences of as much as 50% at 100 MeV with the approximation shown in Fig. 7 of Ref. [13]. This improvement is due entirely to the new mean excitation energies. On the other hand for the lower three curves, for elastic scattering of Li ions, there is excellent agreement for Li⁺², while the approximate formula of Eq. (23a) overestimates the energy loss for elastic scattering of Li⁺⁰ and Li⁺¹. This is a consequence of $I(b,a,1)$ being lower than I_b for Zn.

In Table III I show similar calculations for Li ions on Au. The detailed results for Au are similar in origin to those for

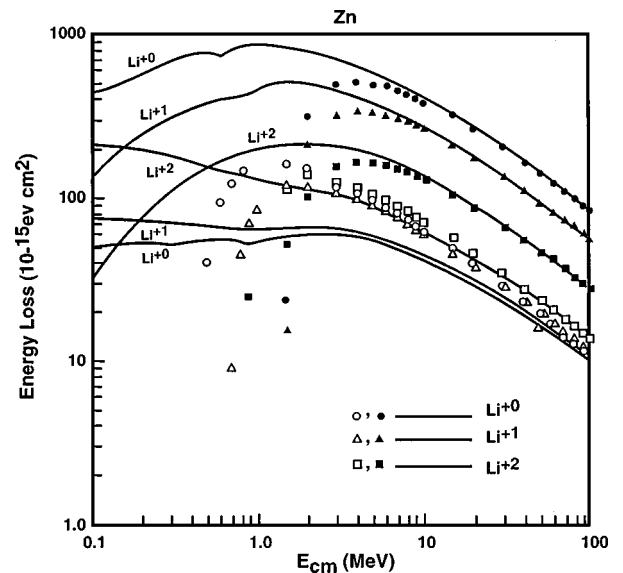


FIG. 4. A comparison of the explicit calculation of energy loss for elastic scattering of one ion plus ionization and excitation of the other ion with the analytic results (circles, triangles, and squares) from Eq. (23a). The solid points are for elastic scattering of Zn, and the open points for elastic scattering of Li ions.

TABLE III. Values of the subshell parameters I_{nl}^{es} calculated with the ionization energy of the ion and the modified elastic scattering factor of the other for Li ions on Au. The generalized mean excitation energies, $I(a,b,j)$ and $I(b,a,j)$ are also listed.

Level \ Ion or Atom	Li ⁺²	Au	Li ⁺¹	Au	Li ⁺⁰	Au
1s	1027.8	808.75	1027.6	827.80	1027.6	824.53
2s		233.90		280.11	1027.6	274.98
2p		222.20		273.57		269.32
3s		133.59		203.91		188.40
3p		150.97		208.76		185.37
3d		208.40		220.17		180.74
4s		80.95		174.67		155.61
4p		96.17		182.25		153.88
4d		129.24		194.23		151.63
4f		83 0674.0		361.67		148.73
5s		31.14		137.19		148.78
5p		30.30		137.57		148.17
5d		71 7099.0		400.84		147.96
6s		506.70		237.14		147.95
$I(\dots)/I(\dots 2)$	1027.8/ 1027.8	1843.4/ 13 426.0	1027.6/ 1033.5	251.01/ 288.82	1027.6/ 1033.5	173.94/ 164.73

Zn. The 4f and 5d levels show an enormous increase in I_{nl}^{es} with increasing degree of ionization. The numerical results on energy loss due to elastic scattering of one ion and ionization and excitation of the other for Li ions on Au are shown as solid lines in Fig. 5. The open and solid circles, triangles, and squares are obtained with Eq. (23a). For the three upper curves, for elastic scattering of Au, the results with the approximate energy loss expression of Eq. (23a) (solid circles, triangles, and squares) are in excellent agreement with the numerical results above the peak in the approximate expression at 10 MeV. This should be compared with differences of as much as a factor of 2 at 100 MeV with the approximation shown in Fig. 10 of Ref. [13]. For the

lower three curves, for elastic scattering of Li⁺⁰ and Li⁺¹ the approximate expression overestimates the energy loss by a factor of 2 at 10 MeV and by 20% at 100 MeV. For Li⁺² the agreement is better than 25% above 4 MeV. In comparing the lower curves in Fig. 5 with the curves using a simpler model shown in Fig. 10 of Ref. [13], one might conclude that the simpler model is a better approximation. In Fig. 6 I show a continuation of the calculations to the 100–1000-MeV regime. The curves are the explicit calculations with the Li ions being elastically scattered, the open circles, triangles, and squares are obtained using Eq. (23a), and the solid circles, triangles, and squares are obtained from Ref. [13]. It is seen that the results with the simple expression of Ref. [13] drift below the explicit results, while there is improved agreement between the results of Eq. (23a) and the explicit calculations at high energy. The explanation appears to be in

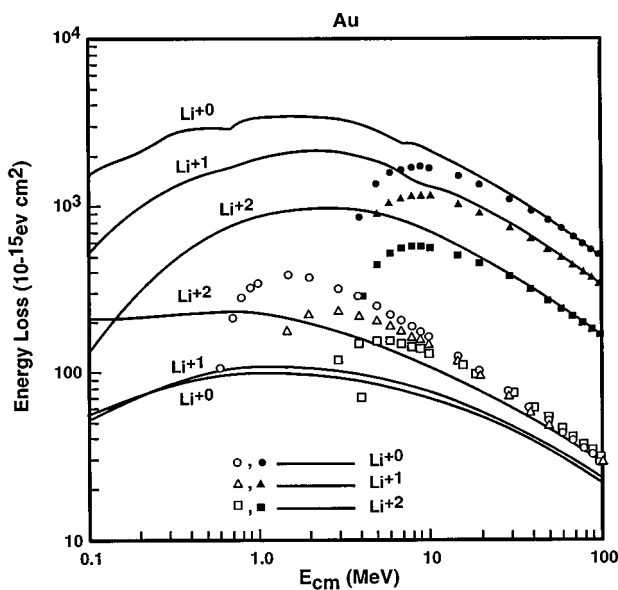


FIG. 5. A comparison of the explicit calculation of energy loss for elastic scattering of one ion plus ionization and excitation of the other ion with the analytic results (circles, triangles, and squares) from Eq. (23a). The solid points are for elastic scattering of Au, and the open points for elastic scattering of Li ions.

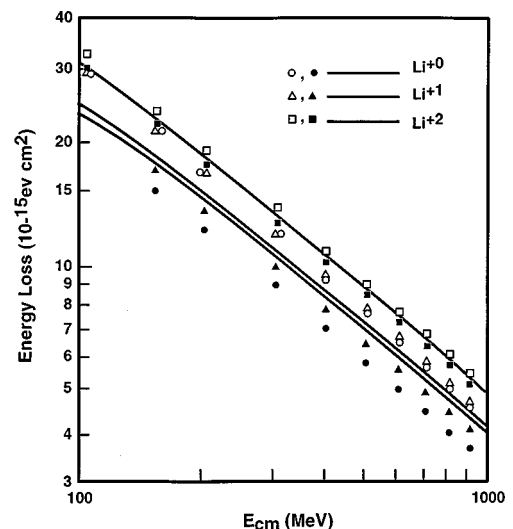


FIG. 6. Results of Fig. (5) for elastic scattering of Au, extended to 1000 MeV. The open circles, triangles, and squares are from Eq. (23a), while the solid circles, triangles, and squares are from Ref. [13].

the explicit calculations; for Li ions the L -shell ionization cross section peaks at 15 MeV, and the K -shell ionization cross section peaks at 150 MeV, indicating than 100 MeV may not be in the asymptotic regime.

VI. DISCUSSION

Results similar to these have been obtained by Kim and Cheng [15], and by Crawford [16]. However, in both papers there is an error that trivializes the SP calculation. For example, in their Eq. (17) Kim and Cheng [15] have an integral

$$\int_a^b f(q) \frac{dq}{q}, \quad (26a)$$

where $f(0)$ is not zero. Writing this as

$$\begin{aligned} & \int_a^b [f(q) - f(0)] \frac{dq}{q} + \int_a^b [f(0)] \frac{dq}{q} \\ &= \int_a^b f(q) \frac{dq}{q} + f(0) \ln(b/a) \end{aligned} \quad (26b)$$

and assuming that

$$\int_0^a [f(q) - f(0)] \frac{dq}{q} = O(a) = O(1/E_p), \quad (26c)$$

then adding Eq. (26c) to Eq. (26b) one has

$$\begin{aligned} \int_a^b f(q) \frac{dq}{q} &= \int_0^b [f(q) - f(0)] \frac{dq}{q} + f(0) \ln(b/a) \\ &\quad - O(1/E_p), \end{aligned} \quad (26d)$$

where a appears only in the log term. With Eq. (26d) [their Eq. (19)] Kim and Cheng [15] are able to immediately do the sum rule and the rest is trivial. There is no involvement of shell structure except through a in the log term. However,

both qualities in Eq. (26c), obtained by assuming that a is small, are incorrect. a is not small. a is $K^2|_{\min}$ in Eq. (3c), and at $\varepsilon_{\max} = E_p - E_{nl}$, $a_{\max} = M_p E_p M_e$. This is also the minimum value of $b = K^2|_{\max}$ at the same ε_{\max} , i.e., the upper and lower limits on the momentum transfer integral define a smooth curve. But, in fact, one can use some knowledge of $f(q)$ to find a lower maximum for a . For a sharply peaked Bethe ridge one can argue that the maximum a is determined as the value at which $K^2|_{\min}$ intersects the Bethe ridge. But this cannot be small since the Bethe ridge extends to infinity. An estimate is found by setting $a_{\max} = \varepsilon$ which leads to

$$a_{\max} = \left(\frac{4m_e}{M_p} \right) E_p,$$

which is also large, since E_p can be large. Thus Eq. (26c) is never valid for calculating SP, certainly not in the limit $E_p \rightarrow \infty$.

Because of the effect of the sum rules in the SP formula one can get the leading term with a poor calculation, i.e., the leading term in the first part of Eq. (24) is

$$(Z_b - z_b) [(z_a)^2 + (Z_a)^2] \ln(4m_e E_r / M_r) \quad (27a)$$

and is also the leading term in Eq. (24) of Kim and Cheng [15]. However, it is also the leading term in the SP approximation in Ref. [13] that merely assumes the dominance of elastic scattering plus ionization and the requirement that the result reproduce the proton results, i.e., the leading term is obtained with a poor calculation. The second term in the first part of Eq. (24) is

$$\begin{aligned} & (Z_b - z_b) \{ - (z_a)^2 \ln[I(b)^2 / I(a, b, 2)] - (Z_a)^2 \ln[I(a, b, 1)] \} \\ &= - (Z_b - z_b) \{ 2(z_a)^2 \ln(I_b) + (Z_a)^2 \ln[I(a, b, 1)] \\ &\quad - (z_a)^2 \ln[I(a, b, 2)] \}. \end{aligned} \quad (27b)$$

The first term in Eq. (27b) agrees with Kim and Cheng [15], but the second term,

$$\begin{aligned} & - (Z_b - z_b) \{ (Z_a)^2 \ln[I(a, b, 1)] - (z_a)^2 \ln[I(a, b, 2)] \} = - (Z_a)^2 \sum_{nl} N_{nl} \ln(I_{nl}^{es}) + (z_a)^2 \sum_{nl} Z_{nl}(0) \ln(I_{nl}^{es}) \\ &= - \sum_{nl} \left\{ [N_{nl}(Z_a)^2 - (z_a)^2 Z_{nl}(0)] \ln(Q_{nl}) \right. \\ &\quad \left. + N_{nl} \int_{Q_{nl}}^{E_B} (dq^2/q^2) [(Z_a)^2 - |Z_a - F_a(q^2)|^2] \right\}, \end{aligned} \quad (27c)$$

should be compared with the second term in Kim and Cheng [15]

$$\begin{aligned} & - (Z_b - z_b) [(z_a)^2 + (Z_a)^2] \ln(G_F) = - (Z_b - z_b) \left\{ \int_1^\infty (dq^2/q^2) [(Z_a)^2 - |Z_a - F_a(q^2)|^2] \right. \\ &\quad \left. - \int_0^1 (dq^2/q^2) [|Z_a - F_a(q^2)|^2 - (z_a)^2] \right\}. \end{aligned} \quad (27d)$$

For the case of unstructured projectiles, where $Z_a = z_a$ and $F(q^2) = 0$, both Eq. (27d) and Eq. (27c) are zero, immediately in Eq. (27d), and in Eq. (27c) by the argument given in Sec. II, but so is the poor approximation given in Ref. [13], since it is designed to reproduce the proton results. However, in general, Eqs. (27c) and (27d) are unlikely to be related, as Eq. (27d) depends on the target only through the $Z_b - z_b$ multiplier, while in Eq. (27c) there is both the $Z_b - z_b$ multiplier and the dependence on the limit on the integral, Q_{nl} , which depends on the subshells of the target (b).

VII. CONCLUSIONS

In Sec. II I gave a direct proof of the assertion that the Bethe mean excitation energy calculated with optical oscillator strengths is the same Bethe mean excitation energy that appears in stopping power formula. Peek [12] had earlier given a proof using distribution theory to extract the finite part of infinite integrals. The advantage of the direct proof is twofold. First, one has an explicit criterion as to when asymptotia is reached. In Sec. III I applied the asymptotic criterion to Al, finding a proton energy of 1 GeV. Clearly this asymptotic criterion is conservative. Second, the direct technique can be applied with confidence to more complicated asymptotic calculations. In particular, it allowed us to generalize the Bethe formula for structureless projectiles interacting with targets, to structured projectiles interacting with targets. In Sec. V I compared the generalized Bethe formula with explicit calculations for Li ions interacting with neutral Zn and Au. In the plane wave Born approximation, the energy loss in these collisions is dominated by collisions where one of the ions is elastically scattered and the other excited or ionized. The generalized Bethe formula for the energy loss was found to be in excellent agreement with the dominant of the two processes, where the heavier ion is elastically scattered. For the second process, where the lighter ion is elastically scattered, the generalized Bethe formula tended to overestimate the energy loss. It was hypothesized that the cause of this is that the PWBA calculations are not asymptotic. To all this one must add the caveat that because of the large cross sections for elastically scattering the heavier ion and ionizing the lighter projectile, the lighter projectile is rapidly stripped of electrons, and a scaled proton treatment may suffice. However, this is true only when the lighter ion is the projectile, suffering multiple collisions. The results here are valid for Zn and Au incident on a Li target. Application of these techniques to heavy ion projectiles are planned for the future.

ACKNOWLEDGMENTS

This work was supported by the United States Department of Energy under Contract No. DE-AC04-94AL85000. San-

dia is a multiprogram laboratory operated by Sandia Corporation, a Lockheed Martin Company, for the United States Department of Energy. The paper benefitted from an exchange of views with Dr. O. Crawford of ORNL.

APPENDIX

The normalized quadrupole calculations of Fig. 3 can be fitted roughly by the curve

$$F(x) = 6x/(6x + |1 - 2x|^3) \quad (\text{A1})$$

and the integral in Eq. (13b) can be written as

$$\begin{aligned} Q(n'l', nl, y) &= \int_0^y (dx/x) F(x) \\ &= \int_0^y (dx/x) \{6x/[6x + (1 - 2x)^3]\} \end{aligned} \quad (\text{A2a})$$

if $y \leq 1/2$, and

$$\begin{aligned} Q(n'l', nl, y) &= \int_0^{1/2} (dx/x) \{6x/[6x + (1 - 2x)^3]\} \\ &\quad + \int_{1/2}^y (dx/x) \{6x/[6x + (2x - 1)^3]\} \end{aligned} \quad (\text{A2b})$$

if $y \geq 1/2$. With the change of variables $1 - 2x = Z$ in the first integral and $2x - 1 = Z$ in the second, the denominator in the integrals are $Z^3 - 3Z + 3$, and $Z^3 + 3Z + 3$, which can be factored into $(Z + Z_0)(Z^2 - ZZ_0 + S)$ with $Z_0 = 2.1038$ and $S = (Z_0)^2 - 3$ in the first integral, and $Z_0 = 0.81773$ and $S = 3 + (Z_0)^2$ in the second integral. Then with the substitution $w = Z + Z_0$, one can rewrite the integrals in Eqs. (A2a) and (A2b) as the integral

$$I = 3 \int_L^U (dw/w) 1/\{w^2 - 3Z_0w + 3[(Z_0)^2 \pm 1]\} \quad (\text{A3})$$

where the plus sign is for the second integral and the minus sign for the first. This is a tabulated integral so

$$\begin{aligned} I &= (1/2 \{2[(Z_0)^2 \pm 1]\}) \ln\{w^2/[w^2 - 3Z_0w + 3[(Z_0)^2 \pm 1]]\} \\ &\quad + 6\{Z_0/[3(Z_0)^2 \pm 12]\}^{1/2} \\ &\quad a \tan\{(2W - 3Z_0)/[3(Z_0)^2 \pm 12]^{1/2}\} \Big|_L^U. \end{aligned} \quad (\text{A4})$$

- [1] H. A. Bethe, Ann. Phys. (Leipzig) **5**, 325 (1930); Z. Phys. D **76**, 293 (1932).
 [2] J. L. Dehmer, M. Inokuti, and R. P. Saxon, Phys. Rev. A **12**, 102 (1975).

- [3] E. J. McGuire, J. M. Peek, and L. C. Pitchford, Phys. Rev. A **26**, 1318 (1982).
 [4] E. J. McGuire, Phys. Rev. A **28**, 2096 (1983).
 [5] H. Sorensen and H. H. Andersen, Phys. Rev. B **8**, 1854 (1973).

- [6] H. H. Andersen, J. F. Bak, H. Knudsen, and B. R. Nielson, *Phys. Rev. A* **16**, 1929 (1977).
- [7] R. Ishiwari, N. Shiomi, and N. Sakamoto, *Phys. Lett.* **75A**, 112 (1979).
- [8] E. J. McGuire, *Phys. Rev. A* **28**, 49 (1982); **28**, 53 (1983).
- [9] E. J. McGuire, *Phys. Rev. A* **26**, 1871 (1982); **28**, 57 (1983).
- [10] H. A. Bethe, L. M. Brown, and M. C. Walske, *Phys. Rev.* **79**, 413 (1950).
- [11] A. Dalgarno, in *Atomic and Molecular Processes*, edited by D. R. Bates (Academic Press, New York, 1962).
- [12] J. M. Peek, *Phys. Rev. A* **27**, 2384 (1983).
- [13] E. J. McGuire, *Phys. Rev. A* **56**, 488 (1997).
- [14] E. J. McGuire, *Laser Part. Beams* **13**, 321 (1995).
- [15] Y.-K. Kim and K.-t. Cheng, *Phys. Rev. A* **22**, 61 (1980).
- [16] O. H. Crawford, *Phys. Rev. A* **39**, 4432 (1989).